

Supplementary Information

Nitrogen-doped carbon nets with micro/mesoporous structure as electrodes for high-performance supercapacitor

Li-Na Han, Xiao Wei,* Qian-Cheng Zhu, Shu-Mao Xu, Kai-Xue Wang, Jie-Sheng Chen*

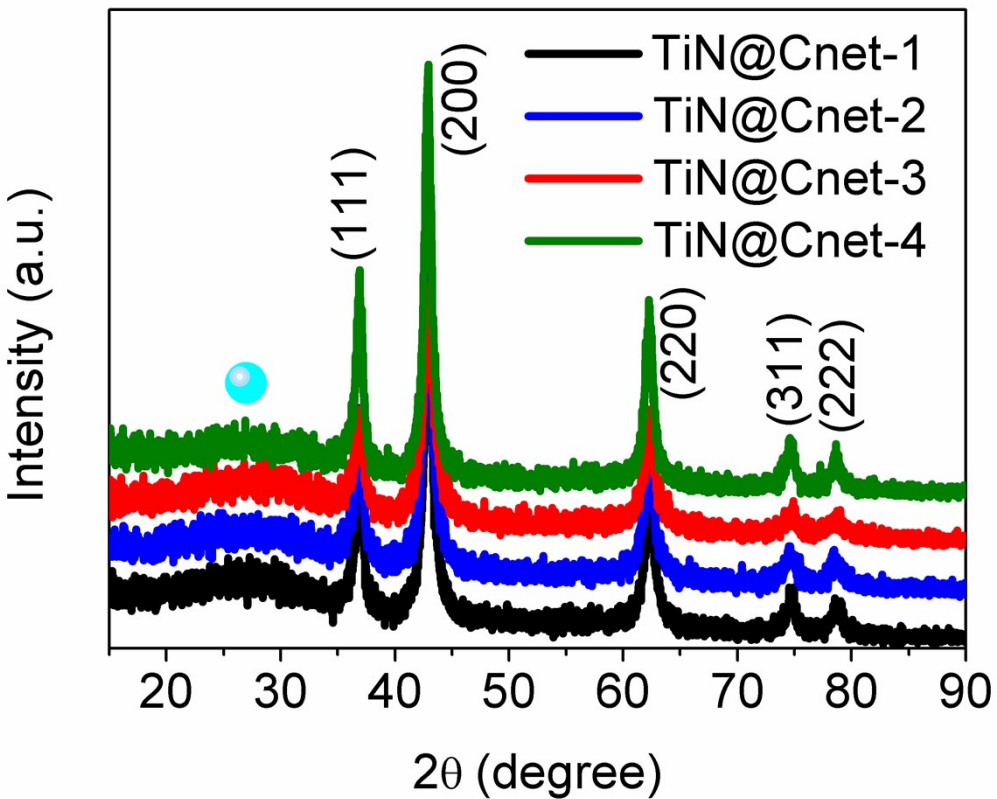


Fig. S1. XRD patterns of TiN/Cnet samples obtained at 800 °C for 1 h with different amount of TTIP and P123. The peak around 26 degrees indicated the existence of carbon components in all the samples. The TiN components exhibited the characteristic diffraction peaks of typical cubic phase TiN (NaCl-type structure, JCPDS No. 38-1420) at 36.91, 43.11, 62.61, 74.11 and 77.91 degrees, ascribed to the crystal planes of (111), (200), (220), (311) and (222), respectively.

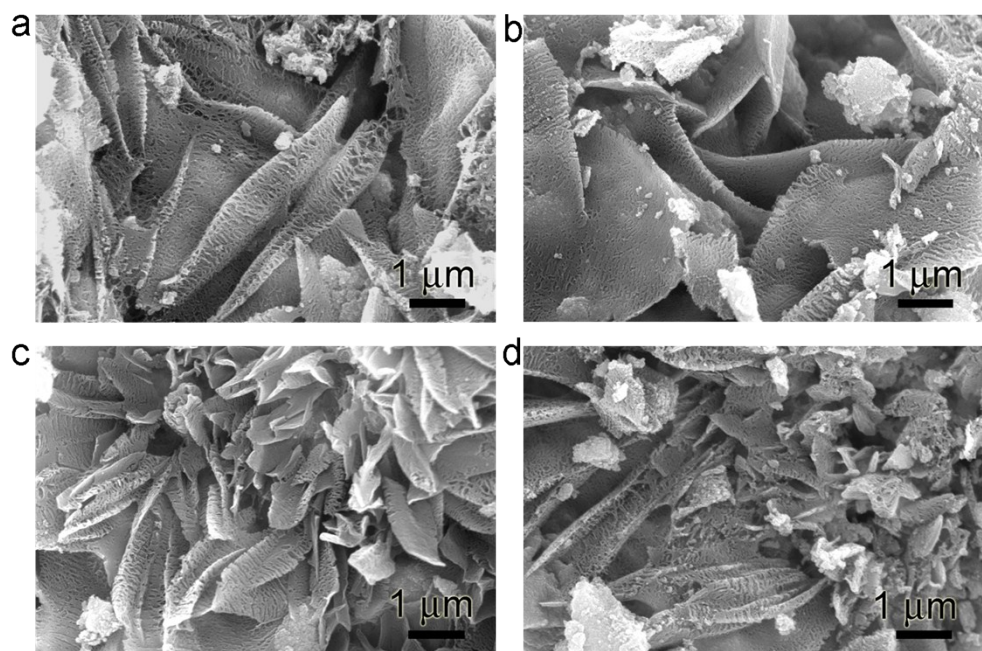


Fig. S2. SEM images of the obtained nitrogen-doped micro/mesoporous carbon materials, (a) N-MM-Cnet-1, (b) N-MM-Cnet-2, (c) N-MM-Cnet-3 and (d) N-MM-Cnet-4.

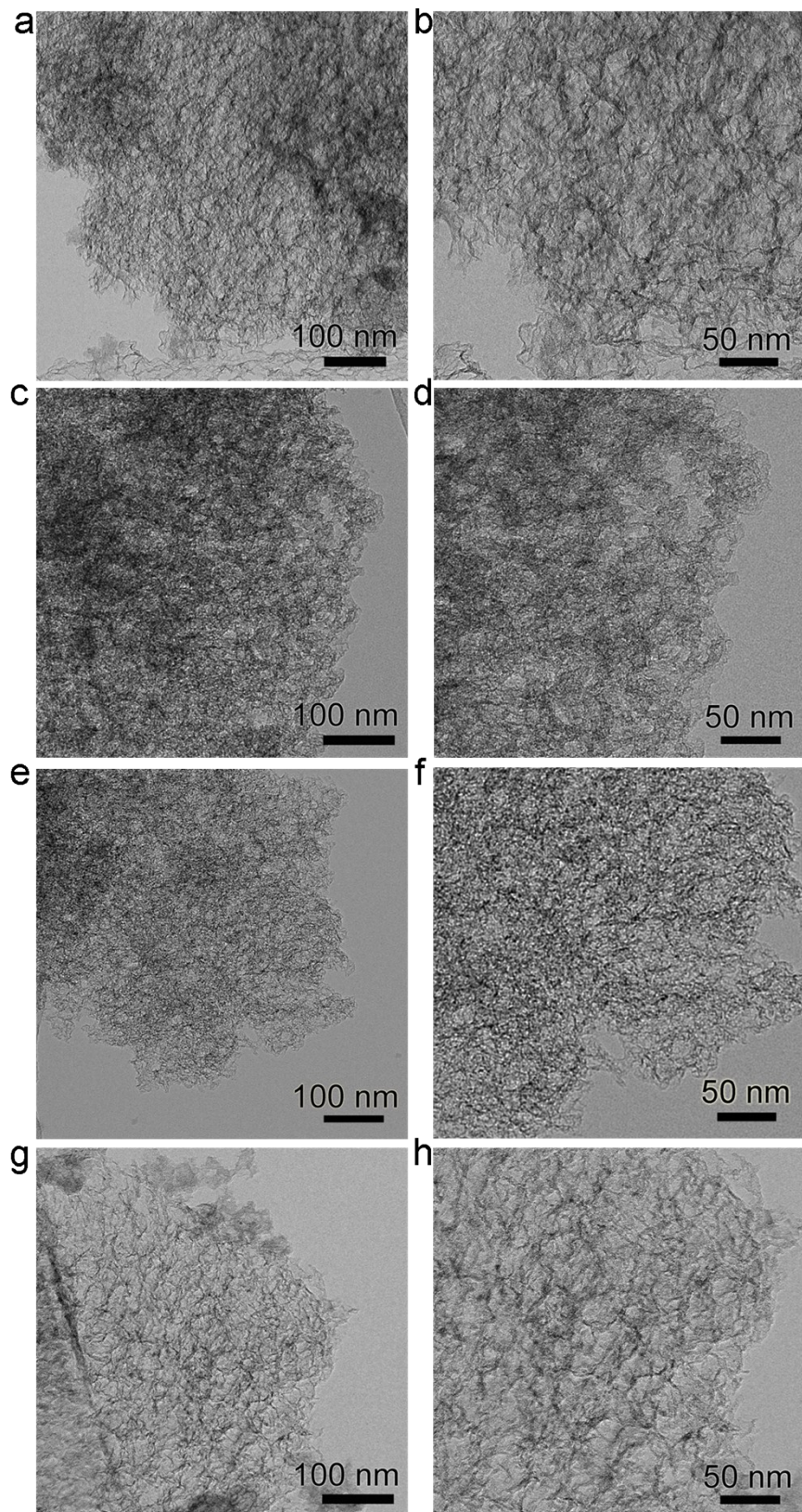


Fig. S3. TEM of the obtained nitrogen-doped micro/mesoporous carbon materials: (a)-(b), N-MM-Cnet-1, (b)-(c) N-MM-Cnet-2, (d)-(e) N-MM-Cnet-3, (g)-(h) N-MM-Cnet-4.

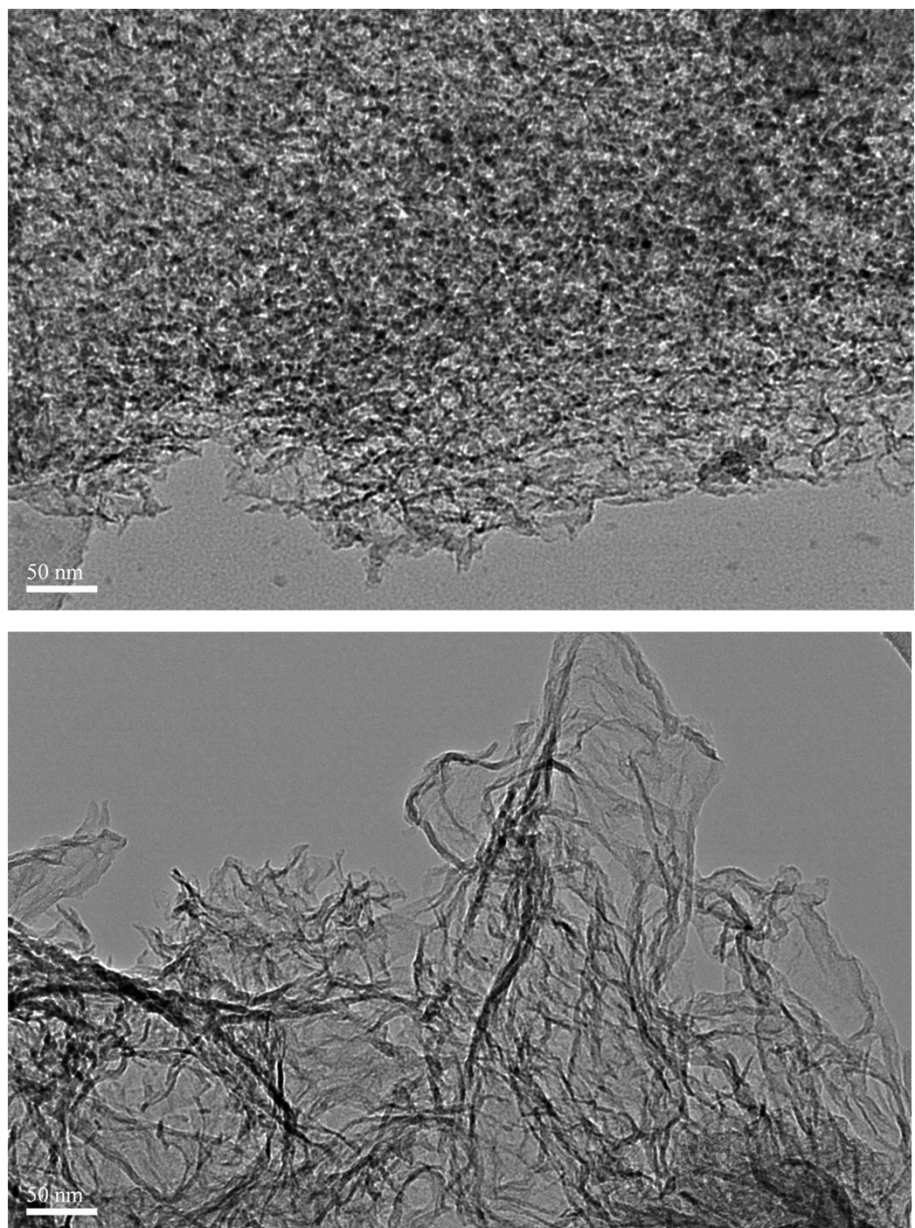


Fig. S4. TEM of N-MM-Cnet-4. Except for carbon net (up), layered carbon (down) formed in N-MM-Cnet-4.

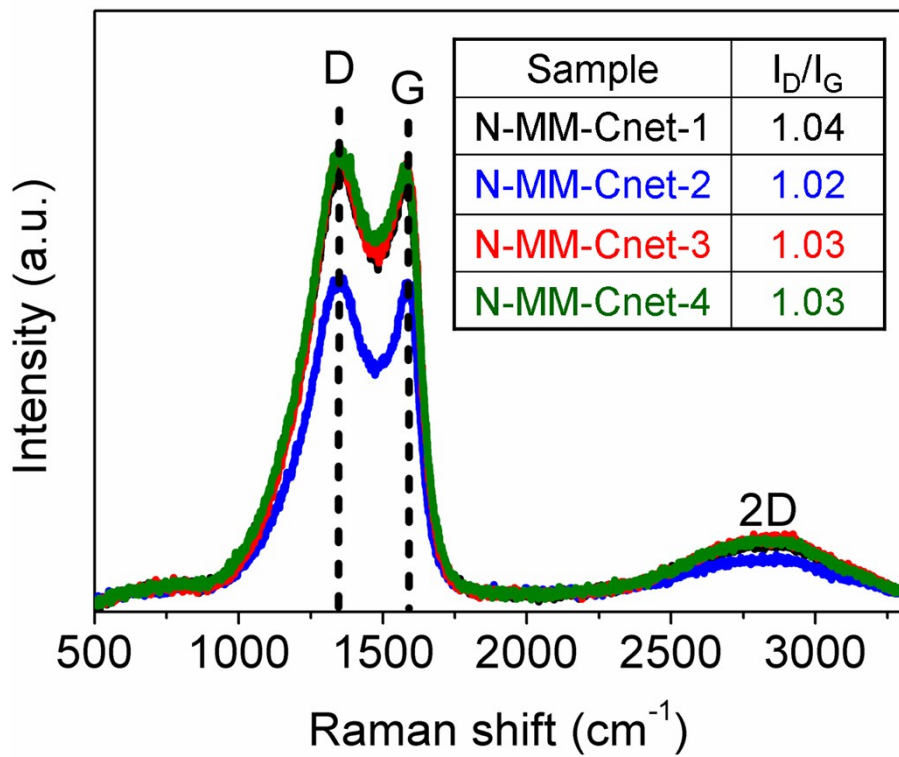


Fig. S5. Raman spectrum of the obtained nitrogen-doped micro/mesoporous carbon nets materials.

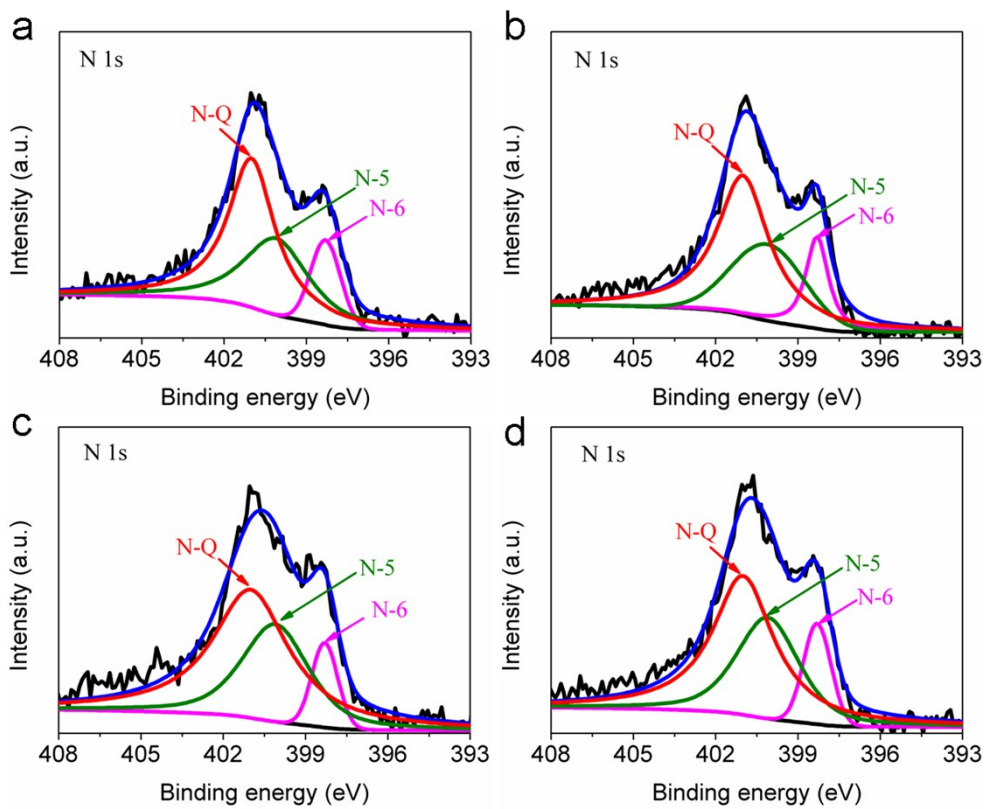


Fig. S6. High-resolution XPS spectra of N1s for nitrogen-doped micro/mesoporous carbon nets: (a) N-MM-Cnet-1, (b) N-MM-Cnet-2, (c) N-MM-Cnet-3 and (d) N-MM-Cnet-4.

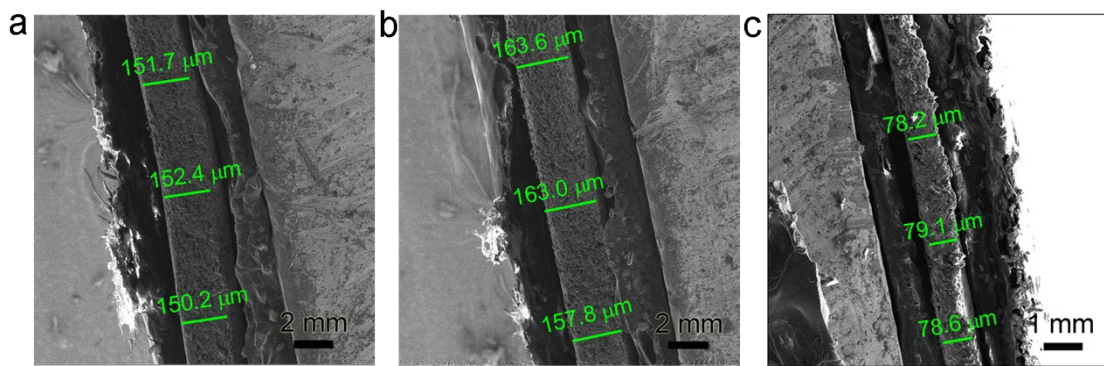


Fig. S7. Cross-sectional SEM images of the N-MM-Cnet-3 film were taken from the same sample with difference area density (a) $8.63 \text{ mg}\cdot\text{cm}^{-2}$, (b) $8.84 \text{ mg}\cdot\text{cm}^{-2}$ and (c) $4.64 \text{ mg}\cdot\text{cm}^{-2}$. The mass density of the N-MM-Cnet-3 film was calculated using a measured area density and an average thickness.⁴⁵ The measurement was repeated several times, and the mass density values were relatively similar. The measured mass density was $0.57 \pm 0.02 \text{ g}\cdot\text{cm}^{-3}$.

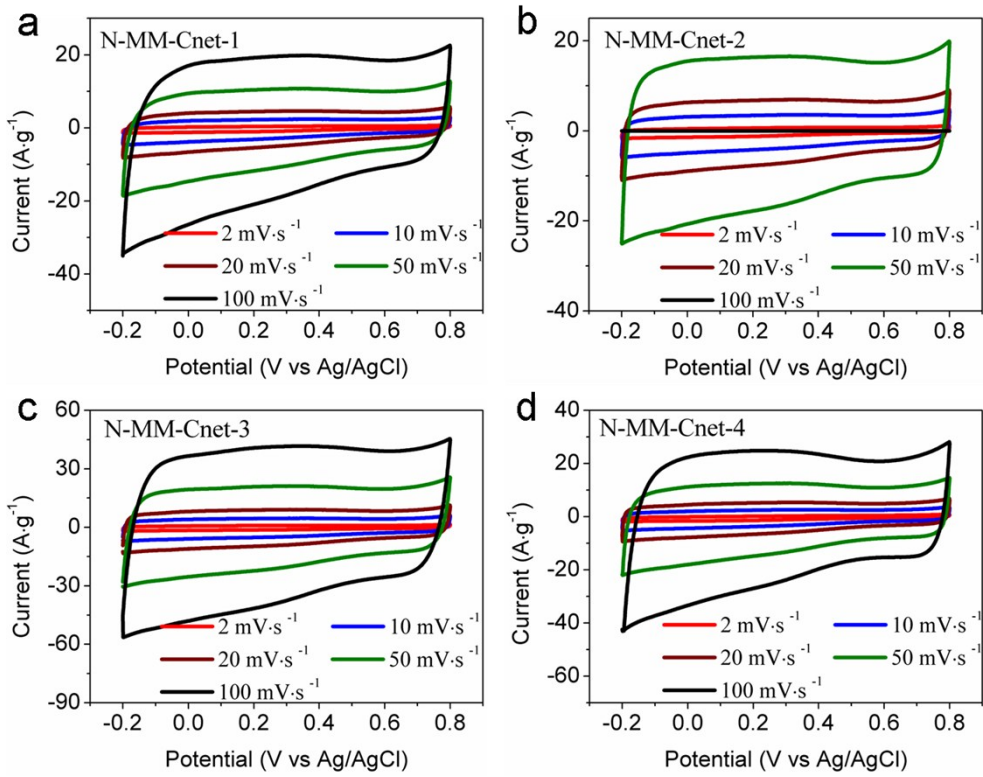


Fig. S8. Cyclic voltammetry (CV) curves of nitrogen-doped micro/mesoporous carbon nets measured at different scan rate from 2 to $100\text{ mV}\cdot\text{s}^{-1}$. (a) N-MM-Cnet-1, (b) N-MM-Cnet-2, (c) N-MM-Cnet-3 and (d) N-MM-Cnet-4.

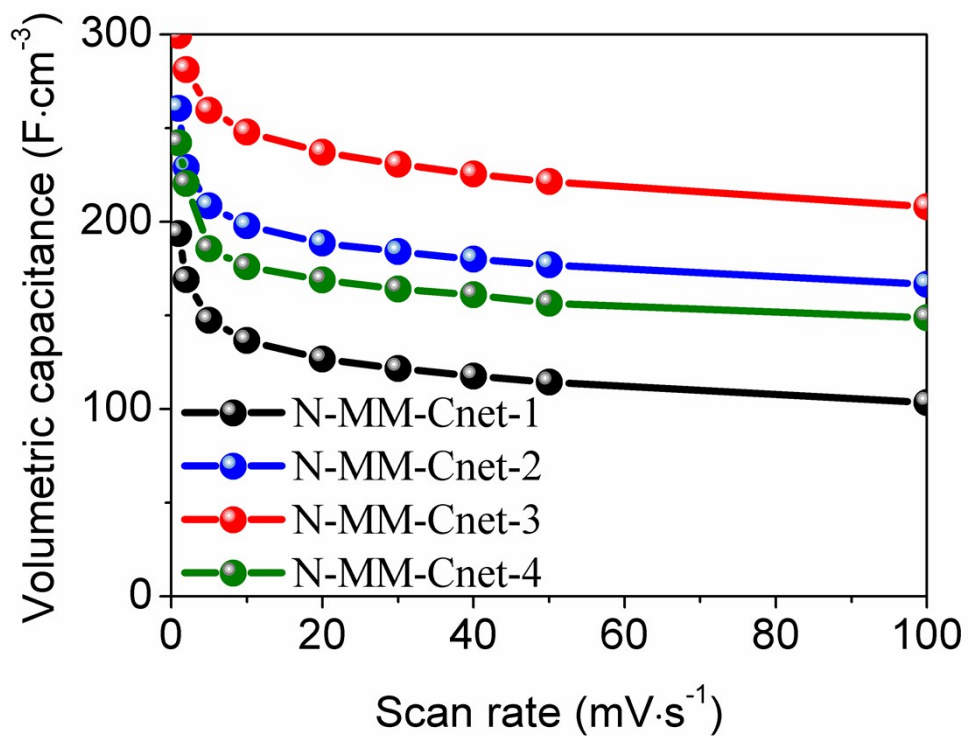


Fig. S9. Volumetric specific capacitances of the samples measured from cyclic voltammetry at different scan rates.

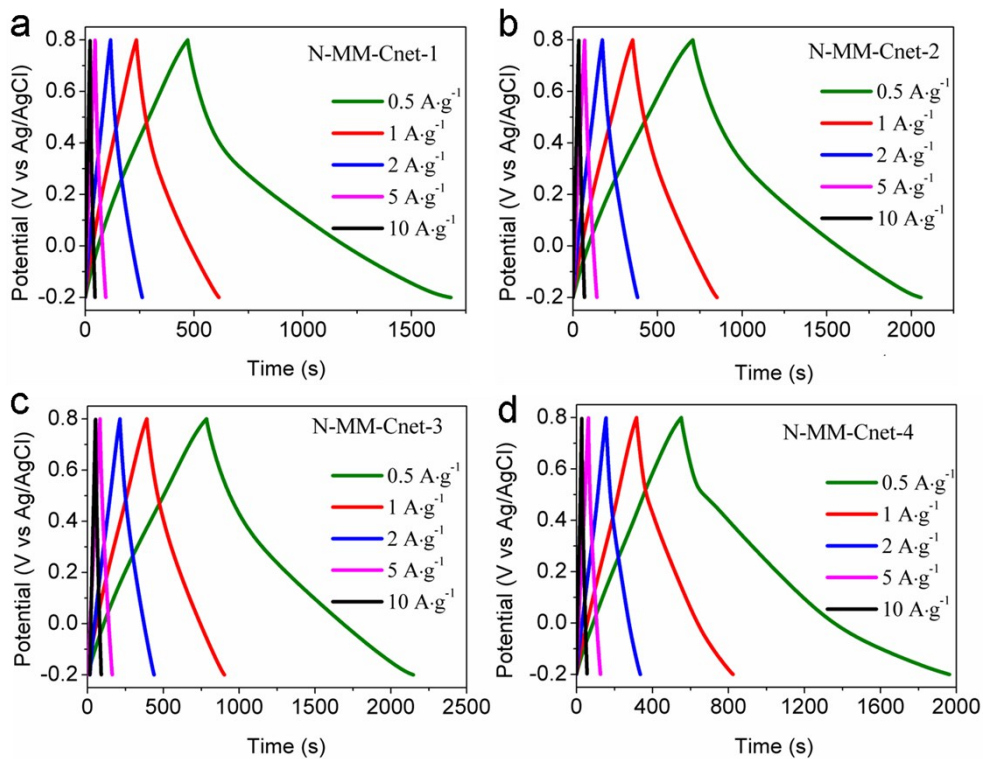


Fig. S10. Galvanostatic charge-discharge (CC) curves of nitrogen-doped micro/mesoporous carbon nets measured at different scan rate from $0.5 \text{ A}\cdot\text{g}^{-1}$. (a) N-MM-Cnet-1, (b) N-MM-Cnet-2, (c) N-MM-Cnet-3 and (d) N-MM-Cnet-4. At lower current density (especially at $0.5 \text{ A}\cdot\text{g}^{-1}$), the constant current charge/discharge plot of N-MM-Cnets show a longer discharge duration is ascribed to the highest contribution of pseudocapacitance.^{S1}

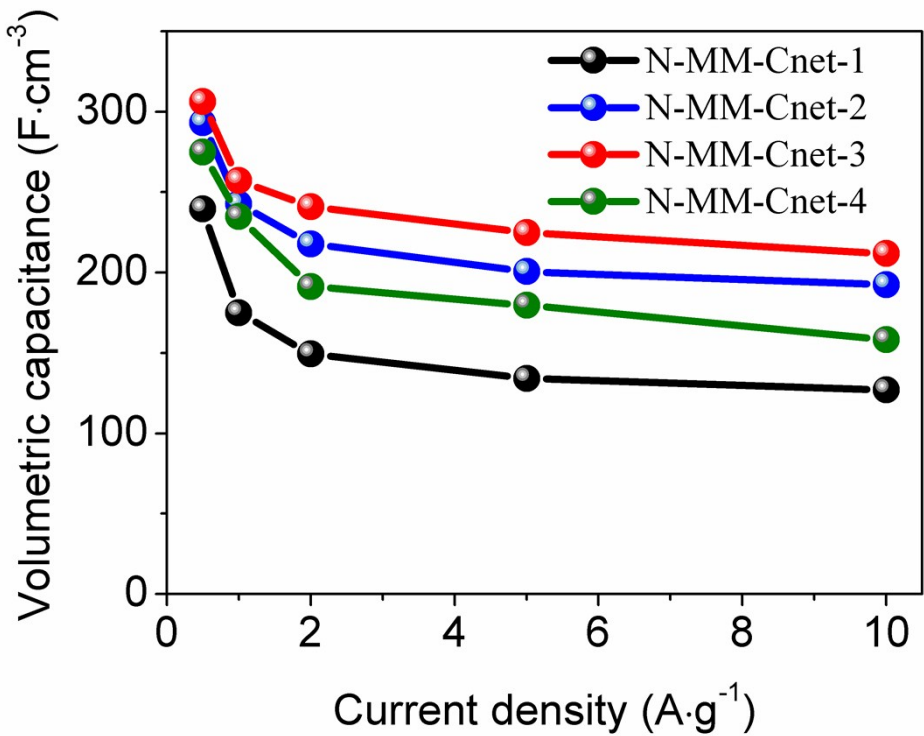


Fig. S11. Volumetric specific capacitances of the samples measured from galvanostatic charge-discharge at different current densities.

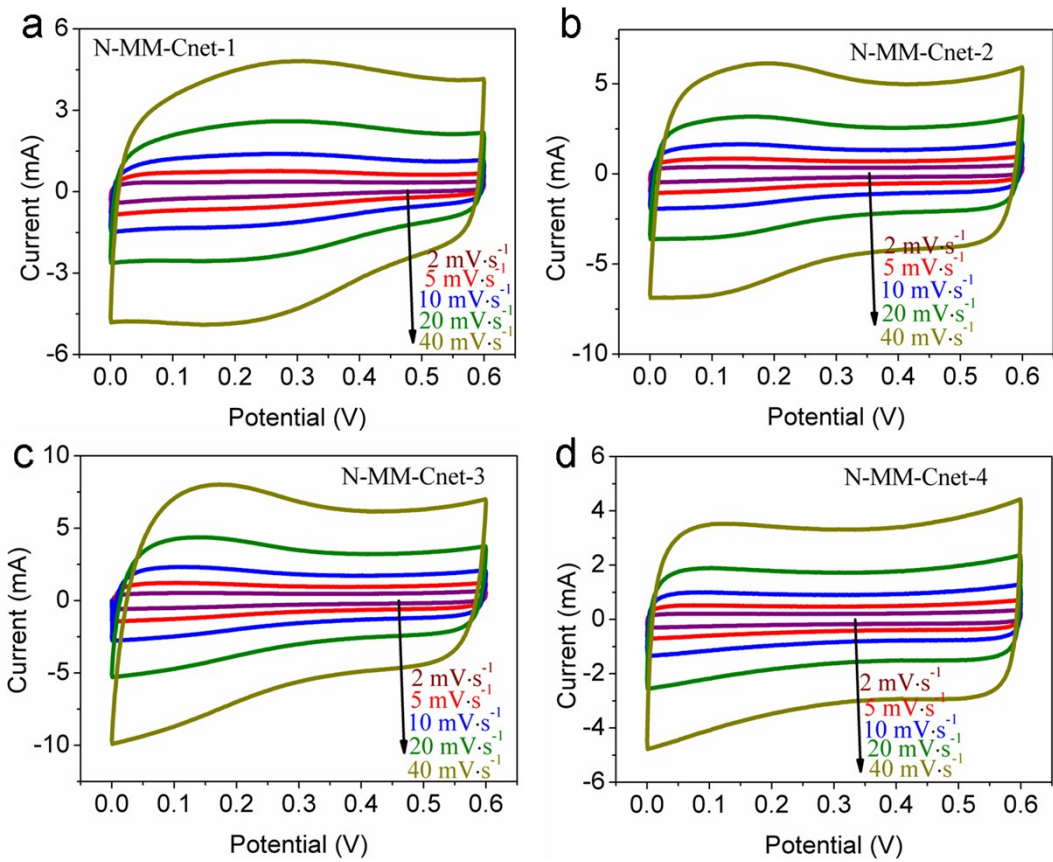


Fig. S12. Cyclic voltammetry (CV) curves of nitrogen-doped micro/mesoporous carbon nets measured at different scan rate from 1 to 40 $\text{mV}\cdot\text{s}^{-1}$ in a symmetric supercapacitor with 0.5 M H_2SO_4 aqueous electrolyte.

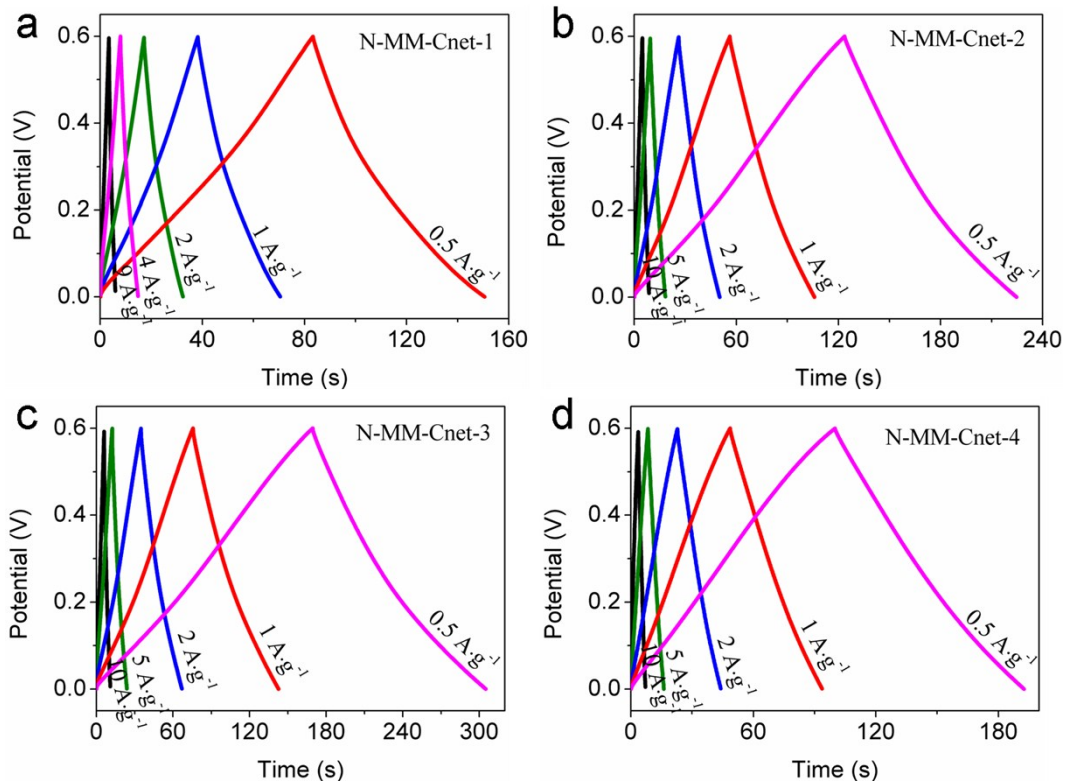


Fig. S13. Galvanostatic charge-discharge (CC) curves of nitrogen-doped micro/mesoporous carbon nets measured at different scan rate from 0.5 to $10\text{ A}\cdot\text{g}^{-1}$ in a symmetric supercapacitor. (a) N-MM-Cnet-1, (b) N-MM-Cnet-2, (c) N-MM-Cnet-3 and (d) N-MM-Cnet-4.

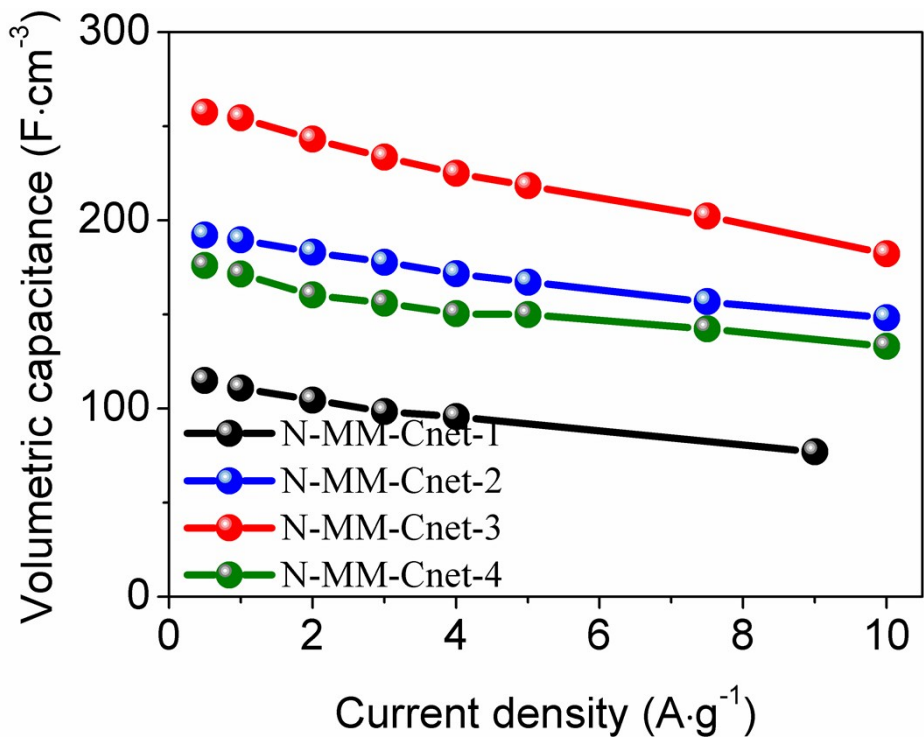


Fig. S14. Volumetric specific capacitances of the samples measured from galvanostatic charge-discharge at different current densities in a symmetric supercapacitor.

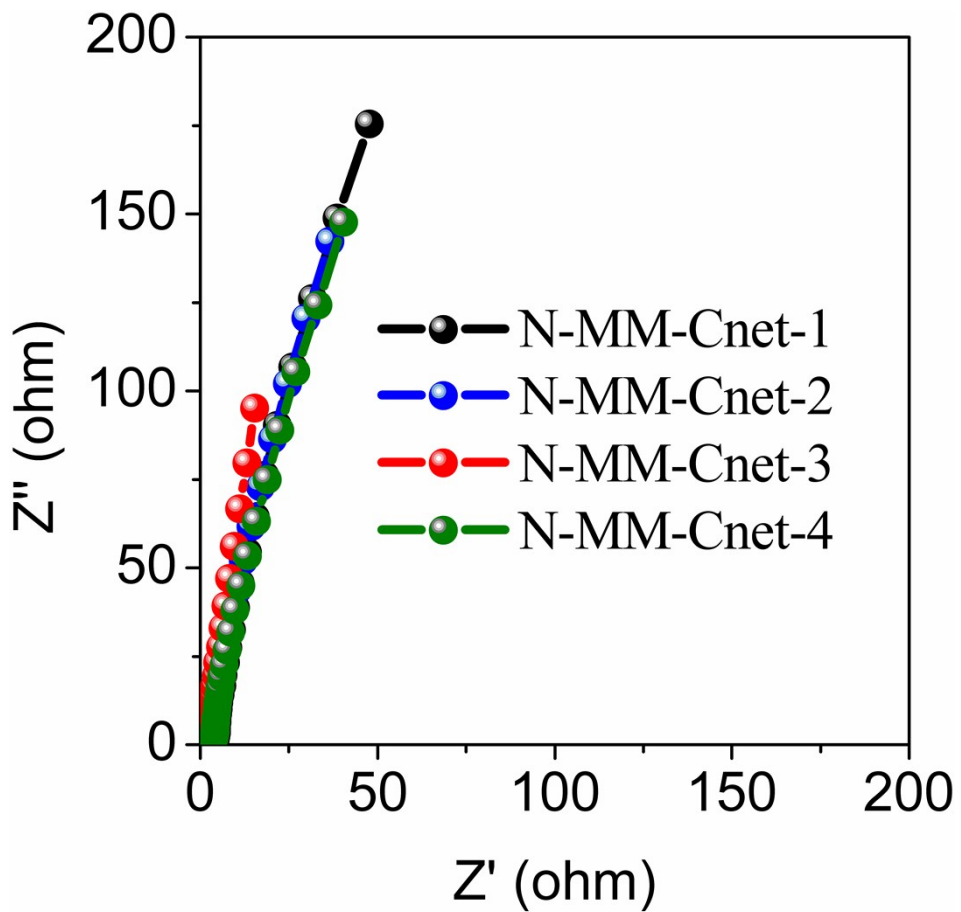


Fig. S15. EIS spectrum of nitrogen-doped micro/mesoporous carbon nets, which was tested in 0.5 M H₂SO₄ with amplitude of 5 mV, from 100 kHz to 0.01 Hz.

Table S1. Synthesis conditions for nitrogen-doped micro/mesoporous carbon nets.

Sample	V _{TTIP} /mL	m _{DCDA} /g	n _{TTIP} /n _{DCDA}	V _{H2O} /mL	V _{HCl} /mL
N-MM-Cnet-1	4.5	3.5	1 : 2.75	4.5	0.72
N-MM-Cnet-2	5	4.2	1 : 2.98	5	0.8
N-MM-Cnet-3	5.5	4.9	1 : 3.14	5.5	0.88
N-MM-Cnet-4	6	5.6	1 : 3.31	6	0.96

Table S2. Pore parameters and chemical compositions (determined by XPS) of N-MM-Cnet materials.

Sample	Compositions			% of total N1s		
	C /%	N /%	O /%	N-Q /%	N-5 /%	N-6 /%
N-MM-Cnet-1	87.36	6.82	5.82	52.98	34.31	12.71
N-MM-Cnet-2	87.57	7.34	5.09	56.27	28.77	14.96
N-MM-Cnet-3	85.16	8.25	6.6	58.46	32.79	8.75
N-MM-Cnet-4	85.18	8.37	6.45	54.60	33.52	11.88

Table S3. Comparison of the electrochemical performance of carbon materials in H₂SO₄ electrolyte reported in literature.

Samples	Specific surface area (m ² ·g ⁻¹)	Electrolyte	Current density (A·g ⁻¹)	Capacitance (F·g ⁻¹)	Ref.
N-MM-Cnet	2144	0.5 M H ₂ SO ₄	0.5	537	This work
porous carbon nanosheets	1890	1 M H ₂ SO ₄	<0.5	<140	S2
porous carbon nanofibers	468.9	0.5 M H ₂ SO ₄	0.2	104	S3
N-doped Carbon	442	1 M H ₂ SO ₄	--	204.8	S4
N-rich CNTs/carbon	352	1 M H ₂ SO ₄	0.05	167.0	S5
CNTs/N-enriched carbon	--	1 M H ₂ SO ₄	--	100	S6
Carbon Nanotube Balls	228.6	0.5 M H ₂ SO ₄	1	100	S7
3D porous rGO film	--	1 M H ₂ SO ₄	1	206	S8
EM-CCG film	--	1 M H ₂ SO ₄	0.1	192	S9
SSG film	--	1 M H ₂ SO ₄	0.1	215	S10
MB-derived ACs	2151	1 M H ₂ SO ₄	0.2	265	S11
HMCS	2144	1 M H ₂ SO ₄	0.25	210	S12
Nitrogen-doped activated carbon	1606	1 M H ₂ SO ₄	5	289	S13
PCNW2	1642	1 M H ₂ SO ₄	1	291	S14
graphene hydrogel	--	1 M H ₂ SO ₄	2	243	S15
Activated graphene	1315	1 M H ₂ SO ₄	0.05	240	S16
Nitrogen-doped porous graphene/carbon	1882.3	1 M H ₂ SO ₄		405	S17
Activated microporous carbon	2557.3	H ₂ SO ₄	0.1	264	S18
CO ₂ -activated macroscopic graphene	829	1 M H ₂ SO ₄	--	278.5	S19

Reference

- S1 S. Dhibar, P. Bhattacharya, G. Hatui, S. Sahoo, C. K. Das, *ACS Sustainable Chem. Eng.* 2014, **2**, 1114-1127.
- S2 A. B. Fuertes and M. Sevilla, *ACS Appl. Mater. Interfaces.*, 2015, **7**, 4344-4353.
- S3 Y. Liu, J. Y. Zhou, L. L. Chen, P. Zhang, W. B. Fu, H. Zhao, Y. F. Ma, X. J. Pan, Z. X. Zhang, W. H. Han and E. Xie, *ACS Appl. Mater. Interfaces.*, 2015, **7**, 23515-23520.
- S4 D. Hulicova, J. Y. Yamashita, Y. Soneda, H. Hatori and M. Kodama, *Chem. Mater.*, 2005, **17**, 1241-1247.
- S5 G. Lota, K. Lota and E. Frackowiak, *Electrochem. Commun.*, 2007, **9**, 1828-1832.
- S6 F. Béguin, K. Szostak, G. Lota and E. Frackowiak, *Adv. Mater.*, 2005, **17**, 2380-2384.
- S7 D.-Y. Kang and J. H. Moon, *ACS Appl. Mater. Interfaces.*, 2014, **6**, 706-711.
- S8 C. Z. Yuan, L. Zhou and L. R. Hou, *Mater. Lett.*, 2014, **124**, 253-255.
- S9 X. W. Yang, C. Cheng, Y. F. Wang, L. Qiu and D. Li, *Science*, 2013, **341**, 534-537.
- S10 X. W. Yang, J. W. Zhu, L. Qiu and D. Li, *Adv. Mater.*, 2011, **23**, 2833-2838.
- S11 J. Yin, Y. Q. Zhu, X. Yue, L. Wang, H. Zhu and C. Y. Wang, *Electrochimica Acta*, 2016, **201**, 96-105.
- S12 D. Liu, G. Cheng, H. Zhao, C. Zeng, D. Y. Qu, L. Xiao, H. L. Tang, Z. Deng, Y. Li and B.-L. Su, *Nano Energy*, 2016, **22**, 255-68.
- S13 F. Gao, J. Y. Qu, Z. B. Zhao, Z. Y. Wang and J. S. Qiu, *Electrochimica Acta*, 2016, **190**, 1134-1141.
- S14 B. Wang, J. H. Qiu, H. X. Feng, E. Sakai and T. Komiyama, *Electrochimica Acta*, 2016, **190**, 229-239.
- S15 L. B. Chen, H. Bai, Z. F. Huang and L. Li, *Energy Environ. Sci.*, 2014, **7**, 1750-1759.
- S16 M. Seredych, M. Koscienska, M. Sliwinska-Bartkowiak and T. J. Bandosz, *ACS Sustainable Chem. Eng.*, 2013, **1**, 1024-1032.
- S17 X. T. Ning, W. B. Zhong, S. C. Li, Y. X. Wang and W. T. Yang, *J. Mater. Chem. A*, 2014, **2**, 8859-8867.
- S18 Y. S. Yun, S. Y. Cho, J. Y. Shim, B. H. Kim, S.-J. Chang, S. J. Baek, Y. S. Huh, *Adv. Mater.*, 2013, **25**, 1993-1998.
- S19 S. Yun, S.-O. Kang, S. J. Park and H. S. Park, *Nanoscale*, 2014, **6**, 5296-5302.